Journal of Marine Research, 59, 977–989, 2001

Effects of topography on the beta-drift of a baroclinic vortex

by Georgi Sutyrin[1]

ABSTRACT

The propagation of compact, surface-intensified vortices over a topographic slope on the beta-plane is studied in the framework of a two-layer model. A perturbation theory is derived for a circular vortex in the upper layer with the lower layer at rest as a basic state. An integral momentum balance for the upper layer is used to obtain expressions for the velocity of the vortex center assuming the flow is quasi-stationary to leading order. This approach allows the calculation of the lower-layer flow pattern as a function of the interface shape and the slope orientation. The essential part of the lower-layer flow pattern is elongated dipolar gyres generated by the cross-slope vortex drift which remains nearly the same as in the reduced-gravity approximation, although it is slightly modified when the slope is not constant. Therefore, the major effect of the lower-layer flow is an additional along-slope propagation which is proportional to the cross-slope speed and the ratio of the interface slope to the topographic slope. Both along-slope and cross-slope drift components are found to be also affected by the slope variation.

1. Introduction

There exists much observational evidences of oceanic eddies influencing the flow over the continental slope; e.g., by Smith (1983) and Evans *et al.* (1985) for Gulf Stream warm core rings approaching the Scotian shelf; by Kirwan *et al.* (1988) and Vukovich and Waddell (1991) for Loop Current rings approaching the Mexican slope; Hamon (1965) and Freeland *et al.* (1986) for East Australian Current eddies approaching the coast, etc. All these studies clearly indicate that the eddy trajectory is significantly modified when it intrudes onto the continental slope and shelf, or moves over a mid-ocean ridge or other topographic feature.

Much of the earlier quasi-geostrophic studies of deep-ocean eddies in flat-bottomed environments is summarized by Flierl (1987) and Korotaev (1997). These studies reveal a tendency for vortices to propagate predominantly westward, with either a northward component for cyclonic eddies or a southward component for anticyclonic eddies. The physical mechanism for the beta-drift of isolated vortices overlying an infinitely deep inactive lower layer has been clarified by Sutyrin (1987) by analyzing the dipolar

1. Graduate School of Oceanography, University of Rhode Island, Narragansett, Rhode Island, 02882, U.S.A.
email: gsutyrin@gso.uri.edu

component of the asymmetric flow generated during the vortex evolution on the beta-plane. An analytical description of the evolution of the dipolar component evolution and corresponding vortex propagation were presented by Reznik and Dewar (1994) for a barotropic model and by Sutyrin and Flierl (1994) for a piecewise constant potential vorticity initial vortex in a reduced-gravity model. This approach has been generalized by Sutyrin and Morel (1997) for a multi-layer model and by Reznik *et al.* (2000) to take into account the next order terms. However, a flow pattern in finite lower layer may significantly enhance the meridional eddy drift (e.g., Flierl, 1984; Chassignet and Cushman-Roisin, 1991; Benilov, 2000; Sutyrin *et al.,* 2001).

There is an analogy between the eddy behavior on a topographic slope and on the beta-plane. We caution here that this analogy only exists in the barotropic limit and only when the effect of the coastal boundary is removed. Firing and Beardsley (1976), Louis and Smith (1982) and Grimshaw *et al.* (1994) demonstrated the rapid dispersion into topographic Rossby waves of eddies over a steep continental slope. Reorganization of the barotropic vortex structure due to even weak topographic effects was considered in a number of laboratory, numerical and theoretical studies, e.g., Carnevale *et al.* (1991), Van Heijst (1994), McDonald (1998), Van Geffen and Davies (1999), Richardson (2000).

However, the ocean is stratified and long-lived eddies are not barotropic, so it is important to understand baroclinic effects. The dynamics of bottom-intensified cold domes on a slope has been intensively studied (e.g., Nof, 1983a; Mory, 1985; Mory *et al.,* 1987; Whitehead *et al.,* 1990; Swaters and Flierl, 1991; Swaters, 1998). On the other hand, oceanic eddies such as Gulf Stream rings are surface-intensified (their main core is not in direct contact with the topography), and their evolution over slope topography is substantially different. Using a two-layer primitive equation numerical model on the beta-plane, Smith and O'Brien (1983) found that the trajectories of eddies interacting with a sloping bottom is different for cyclones and anticyclones: cyclones can penetrate further onto the continental shelf than their anticyclonic counterparts. They also pointed out that the topographic beta-effect tends to cause eddies to move in the direction of the phase propagation of free topographic Rossby waves. In numerical simulations by Smith (1986), eddies with a weak lower-layer circulation rapidly evolve through topographic dispersion to upper layer features. Kamenkovich *et al.* (1996) found that when crossing steep ridges, even large vortices such as Agulhas eddies become compensated (nearly zero deep flow). The trajectory of surface-intensified vortices in a two-layer model over a very steep slope deviates only slightly from the trajectory calculated without the lower-layer feedback (Thierry and Morel, 1999). Sakamoto and Yamagata (1997) also considered a baroclinic vortex translating over an isolated topographic feature from the perspective of so-called JEBAR effect. Finally, topography may also affect the baroclinic stability and formation of vortices, as studied by Hart (1975), LaCasce (1998) and Cenedese and Linden (1999).

Besides the beta-effect, the presence of a vortex companion of opposite sign either in the same layer or beneath the main eddy may play an important role in the vortex evolution (e.g., Nof, 1985; Killworth, 1986; Sutyrin and Dewar, 1992; Dewar and Gaillard, 1994;

Pakyari and Nycander, 1996; Aiki and Yamagata, 2000). Some topographic effects were investigated for dipolar vortices in barotropic models (e.g., Velasko Fuentes and Van Heijst, 1994) and baroclinic models (e.g., Reznik and Sutyrin, 2001). The interaction with the coastal boundary provides an 'image-effect' (i.e. the eddy's advection along a free-slip wall due to its image causing anticyclones to propagate northward along the western boundary) (e.g., Shi and Nof, 1994; Sutyrin *et al.,* 2001).

Nevertheless, the most theoretical progress has been made regarding the vortex evolution over flat bottom, while the basic mechanisms of baroclinic vortex-topography interaction are not well understood. In this paper we suggest an asymptotic theory that describes the basic features of the lower-layer flow beneath the surface-intensified vortex and estimates the effects of a topographic slope on the beta-drift of the vortex center for an arbitrary slope orientation. The two-layer model is described in Section 2. The perturbation theory and integral constraints are described in Section 3. The solution for the cases of a constant slope and a variable slope are considered in Section 4. The discussion and conclusions are presented in Section 5.

2. Two-Layer equations

We consider a two-layer, rotating fluid assuming the Boussinesq, hydrostatic, rigid-lid, and β-plane approximations. The layer density is ρ_j, the depth is h_j, the pressure is p_j, and the velocity vector is $\mathbf{v}_j = (u_j, v_j)$, where $j = 1$ and $j = 2$ represent variables in the upper and the lower layer, respectively.

First, we nondimensionalize the variables as follows:

$$(\hat{X}, \hat{Y}) = (X, Y)/L_R, \quad \hat{t} = tf_0, \quad \hat{f} = f/f_0, \tag{1}$$

$$(\hat{u}_j, \hat{v}_j) = (u_j, v_j)/V_g, \quad \hat{h}_j = h_j/H_1, \quad \hat{p}_j = p_j/\rho_1 V_g^2, \tag{2}$$

where $L_R = V_g/f_0$ is the upper-layer radius of deformation, $V_g = \sqrt{g'H_1}$ is the baroclinic gravity wave speed, H_1 is the characteristic upper layer thickness, f_0 is the Coriolis parameter at the reference latitude, and $g' = (\rho_2 - \rho_1)\, g/\rho_1$ is the reduced gravity.

After dropping the tildes for the nondimensional variables, the momentum and continuity equations become

$$\partial_t \mathbf{v}_j + (\mathbf{v}_j \cdot \nabla)\mathbf{v}_j + f\mathbf{k} \times \mathbf{v}_j = -\nabla p_j, \tag{3}$$

$$\partial_t h_j + \nabla \cdot (h_j \mathbf{v}_j) = 0, \quad h_2 = H(X) - h_1 \tag{4}$$

where ∇ is the horizontal differential operator, and $\mathbf{k}$ is the vertical unit vector. Here we assume $\rho_2 - \rho_1 \ll \rho_1$. The right-hand coordinate system corresponds to the depth topography $H(X)$, with the X-axis directed offshore, and the Y-axis parallel to the isobath. Thus, the dimensionless Coriolis parameter is $f = 1 + \epsilon(-X \sin\theta + Y \cos\theta)$, where θ is the angle measured clockwise from the east to the X-axis, and $\epsilon = \beta L_R/f_0$, β is the

dimensional northward gradient of the Coriolis parameter. The pressure and upper layer thickness gradients are related by the hydrostatic equation:

$$\nabla h_1 = \nabla(p_1 - p_2), \tag{5}$$

Potential vorticity, q_j, is conserved in fluid parcels in each layer:

$$(\partial_t + \mathbf{v}_j \cdot \nabla) q_j = 0, \quad q_j \equiv \frac{f + \mathbf{k} \cdot \nabla \times \mathbf{v}}{h_j}. \tag{6}$$

Typically $\epsilon \simeq 10^{-2}$ and it is considered as a small parameter here.

3. The perturbation theory

When $\epsilon = 0$ (the f-plane) any circular vortex in the upper layer

$$p_1 = h_1 = P(r), \quad \mathbf{v_1} = \mathbf{V_1} = \Omega(r)(-Y, X), \quad \frac{dP}{dr} = r\Omega(1 + \Omega). \tag{7}$$

with no motion in the lower layer ($\mathbf{v_2} = 0$) is a stationary solution of the two-layer system. The β-effect induces the vortex propagation that generates the lower-layer flow which may provide a feedback to the vortex propagation.

Considering an expansion in ϵ, we seek the solution in the coordinate system ($x = X - \epsilon x_0$, $y = Y - \epsilon y_0$), translating with the velocity ($\epsilon \dot{x}_0$, $\epsilon \dot{y}_0$) in the form

$$p_1 = P(r) + \epsilon(\eta + \psi), \quad h_1 = P(r) + \epsilon\eta, \quad \mathbf{v_1} = \Omega(r)(-y, x) + \epsilon\mathbf{v} \tag{8}$$

$$p_2 = \epsilon\psi, \quad h_2 = H(x + \epsilon x_0) - P(r) - \epsilon\eta, \quad \mathbf{v_2} = \epsilon\mathbf{k} \times \nabla\psi. \tag{9}$$

The problem involves multiple time scales (t, ϵt, ...), and here we consider a quasi-stationary flow resulting from the radiation of planetary and topographic Rossby waves away from the vortex. The evolution of the flow field at a slow time scale is out of the scope of this paper.

a. Linearization

The steadily translating perturbation at leading order satisfies the following system obtained by linearizing the original equations.

$$(\mathbf{v} \cdot \nabla)\mathbf{V_1} + (\mathbf{V_1} \cdot \nabla)\mathbf{v} + \mathbf{k} \times \mathbf{v} + \nabla(\eta + \psi) = (x \sin\theta - y \cos\theta)\mathbf{k} \times \mathbf{V_1} + L_0\mathbf{V_1} \tag{10}$$

$$\nabla \cdot (P\mathbf{v} + \eta\mathbf{V_1}) = L_0 P \tag{11}$$

$$J[\psi, H(x) - P(r)] = -L_0 P, \quad L_0 \equiv \dot{x}_0\partial_x + \dot{y}_0\partial_y. \tag{12}$$

We see that the lower-layer flow can be found independently of the upper-layer perturbation. The upper-layer perturbations consist of three parts: the first two, which are proportional to sin θ and cos θ, respectively, describe along-slope and cross-slope

beta-drift of the vortex in the reduced-gravity approximation (RG). They can be found in a similar way to that suggested by Benilov (1996). The third part describes the effect of the lower layer, which also consists of two components, proportional to the cross-slope ($\dot{x}_0$) and along-slope ($\dot{y}_0$) vortex propagation speed.

b. Integral constraints

Actually, it is not necessary to calculate the upper-layer perturbations in order to find the propagation speed: it can be found from integral constraints in a similar way to that suggested by Killworth (1983) and Nof (1983b) assuming the eddy is localized; i.e., the flow decays fast enough with r and all following integrals are finite. First, multiplying the mass conservation equation (11) by x and y, and integrating by parts over the entire area, we obtain

$$M\dot{\mathbf{r}}_\mathbf{0} = \int (P\mathbf{v} + \eta\mathbf{V}_\mathbf{1})dxdy, \quad M = 2\pi \int (P - P_\infty)rdr, \tag{13}$$

where $\dot{\mathbf{r}}_\mathbf{0} = (\dot{x}_0, \dot{y}_0)$ is the propagation velocity vector, and P_∞ is the unperturbed upper-layer depth at the periphery, which can be zero in the case of lens-like vortex.

The momentum perturbation integral in (13) can be expressed using the momentum equation (10) multiplied by P in a combination with (11) multiplied by $\mathbf{V}_\mathbf{1}$ and integrated by parts over the entire area:

$$\int (Pv + \eta V_1)dxdy = \sin\theta \int P\Omega x^2 dxdy + \int P\partial_x\psi dxdy, \tag{14}$$

$$\int (Pu + \eta U_1)dxdy = \cos\theta \int P\Omega y^2 dxdy - \int P\partial_y\psi dxdy. \tag{15}$$

Here we use (7) to express the first integrals on the right-hand side by the sum of the mass excess, M, potential energy, E_p, and kinetic energy, E_k

$$\int P\Omega x^2 dxdy = \int P\Omega y^2 dxdy = -P_\infty M - E, \tag{16}$$

$$E = E_p + E_k, \quad E_p = \pi \int (P - P_\infty)^2 rdr, \quad E_k = \pi \int P\Omega^2 r^3 dr. \tag{17}$$

Therefore, we obtain

$$\dot{x}_0 = -\cos\theta\left(P_\infty + \frac{E}{M}\right) - \frac{1}{M}\int P\partial_y\psi dxdy,$$

$$\dot{y}_0 = -\sin\theta\left(P_\infty + \frac{E}{M}\right) + \frac{1}{M}\int P\partial_x\psi dxdy. \quad (18)$$

Here the first terms describe the beta-drift in RG-approximation found by Killworth (1983) and Nof (1983b). The ratio E/M is positive for anticyclones and negative for cyclones, and provides essential difference between evolution of cyclonic and anticyclonic eddies (e.g., Nezlin and Sutyrin, 1994). The second parts describe the additional drift due to the lower-layer flow feedback which is the focus of this study.

For the lower layer, we multiply (12) by P and integrate over the plane to obtain

$$\int \frac{dH}{dx} P\partial_y\psi dxdy = 0. \quad (19)$$

Thus, in the case of a constant slope, $dH/dx = const$, the lower-layer flow does not affect the cross-slope propagation speed as seen from (18). In order to find the topographic effect on the along-slope propagation speed and the effects of variable slope, we need to consider the lower-layer flow in greater detail.

4. Topographic effects

The first order equation (12) can be easily integrated along characteristics to find an explicit expression for the lower-layer flow pattern, but only when the topographic slope is larger than the interface slope. Therefore, this theory cannot be applied to the flat bottom case which still remains challenging.

First we analyze the along-slope vortex motion when the slope is constant.

a. Constant slope

Assuming $H = H_0 + Sx$, the solution to (12) can be written in the form

$$\psi = \dot{y}_0 \frac{P(r) - P_\infty}{S} - \dot{x}_0 \frac{F(x, y)}{S}, \quad (20)$$

where the function F obeys the following equation

$$J\left(F, x - \frac{P}{S}\right) = \partial_x P. \quad (21)$$

From (20) we see that the first component of the lower-layer flow pattern, which is proportional to the along-slope drift, $\dot{y}_0$, represents a circular eddy. Its streamfunction has

the same sign as upper-layer vortex when $\dot{y}_0 > 0$ and opposite sign when $\dot{y}_0 < 0$. This lower-layer eddy does not affect the vortex drift as seen from (18).

To find the second component of the lower-layer flow from (21), we introduce a coordinate transformation $\zeta = x - P/S$; $\eta = y$ assuming there are no closed isolines of $x - P/S$ and the perturbation decays at $y \to \infty$. Then the solution is expressed as an integral along isolines $\zeta = const$

$$F = \int_{\eta}^{\infty} \partial_{\zeta} P d\eta. \tag{22}$$

This solution has an analogy with the Sverdrup relation for large-scale flow caused by the wind stress: the topography is analogous to the β-effect, while the stretching of the lower layer by the moving interface is analogous to the wind stress curl.

Inserting (20) and (22) into (18) we obtain

$$\dot{x}_0 = -\cos\theta\left(P_{\infty} + \frac{E}{M}\right), \quad \dot{y}_0 = -\sin\theta\left(P_{\infty} + \frac{E}{M}\right) + \dot{x}_0 \frac{S_P}{S}, \tag{23}$$

where

$$S_P = \frac{1}{M}\int F \partial_x P dx dy. \tag{24}$$

Here we see that the effect of the lower-layer flow on the along-slope propagation is proportional to the cross-slope speed and inverse proportional to the slope steepness. The value of S_P is defined mainly by the maximum interface slope in the vortex as we see below.

When the interface slope in the vortex is much less than the topographic slope ($|P'| \ll S$), the expression (22) is simplified and becomes

$$F \approx x \int_{y}^{\infty} \frac{dP}{dr}\frac{dy}{r}, \quad S_P = \frac{1}{2M}\int_{-\infty}^{\infty} F^2_{(y=-\infty)} dx \tag{25}$$

and we see that the second component of the lower-layer flow is antisymmetric: $F(-x) = -F(x)$. Corresponding parts of F describe cyclonic and anticyclonic gyres beneath the vortex which produce additional along-slope vortex propagation according to (23) (Fig. 1).

In particular, for a Gaussian vortex

$$P = P_{\infty} + A\,\exp(-r^2/2R^2), \quad M = 2\pi A R^2, \quad S_P = \kappa \frac{A}{2R} \tag{26}$$

where A/R characterizes the interface slope, and the coefficient $\kappa = \sqrt{\pi}/2 = 0.886$.

If the interface slope is comparable to the topographic slope, the integral (24) can be

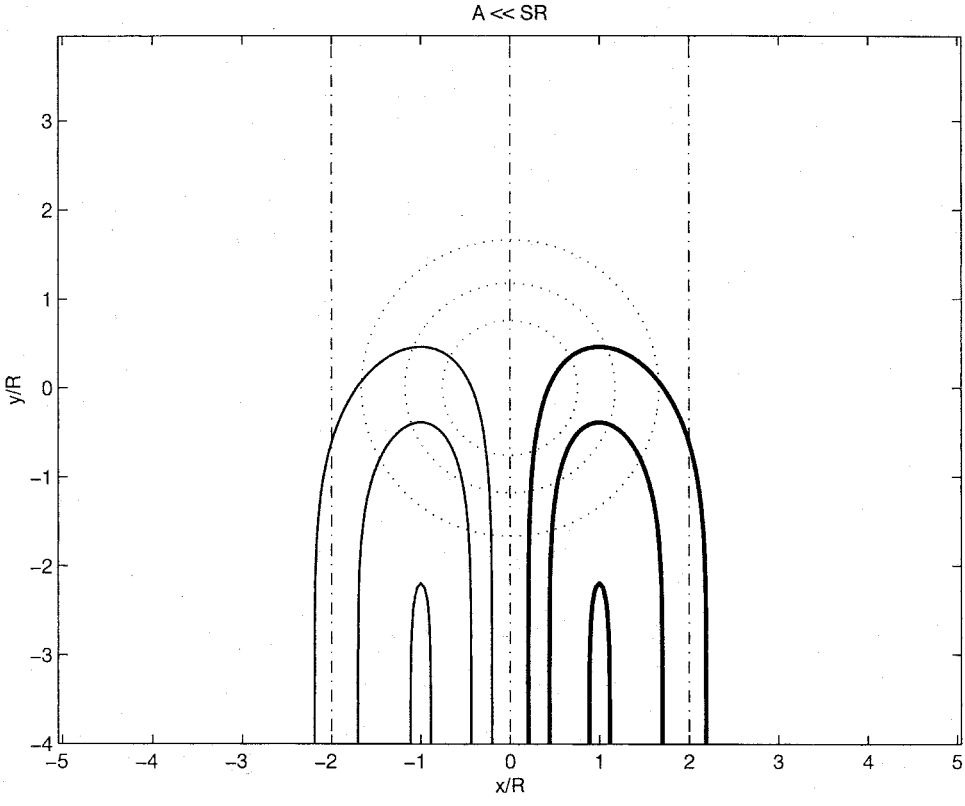

Figure 1. The antisymmetric component of the lower-layer flow, F, described by (25) for a Gaussian vortex (26) superimposed by isolines of the interface, P, (dotted circles) and isolines of x (dash-dotted lines). Thick lines represent cyclonic circulation.

calculated numerically. When the ratio of the interface slope to the topographic slope increases, the curvature of isolines $x - P/S = const$ becomes substantial and the lower-layer gyres lose their antisymmetry: the cyclonic gyre intensifies, while the anticyclonic gyre becomes less intense as shown in Figure 2. However, for a Gaussian vortex the value of $\kappa \equiv 2RS_P/A$ only increases slightly: $\kappa = 1$ when $A/RS = 1$.

These results allow us to describe the topographic effects for an *arbitrary* orientation of the slope. For meridional bathymetry, $\sin\theta = 0$, the westward beta-induced cross-slope vortex motion generates the lower-layer dipolar gyres (as in Fig. 1 and 2) which advects the vortex meridionally. Near a west coast ($\cos\theta = 1$), the effect of continental slope results in the southward advection of anticyclones and northward advection of cyclones, while near an east coast ($\cos\theta = -1$), the topographic slope results in the southward advection of cyclones and northward advection of anticyclones. These topographic effects can be simply explained in terms of potential vorticity conservation in the same way as mentioned above

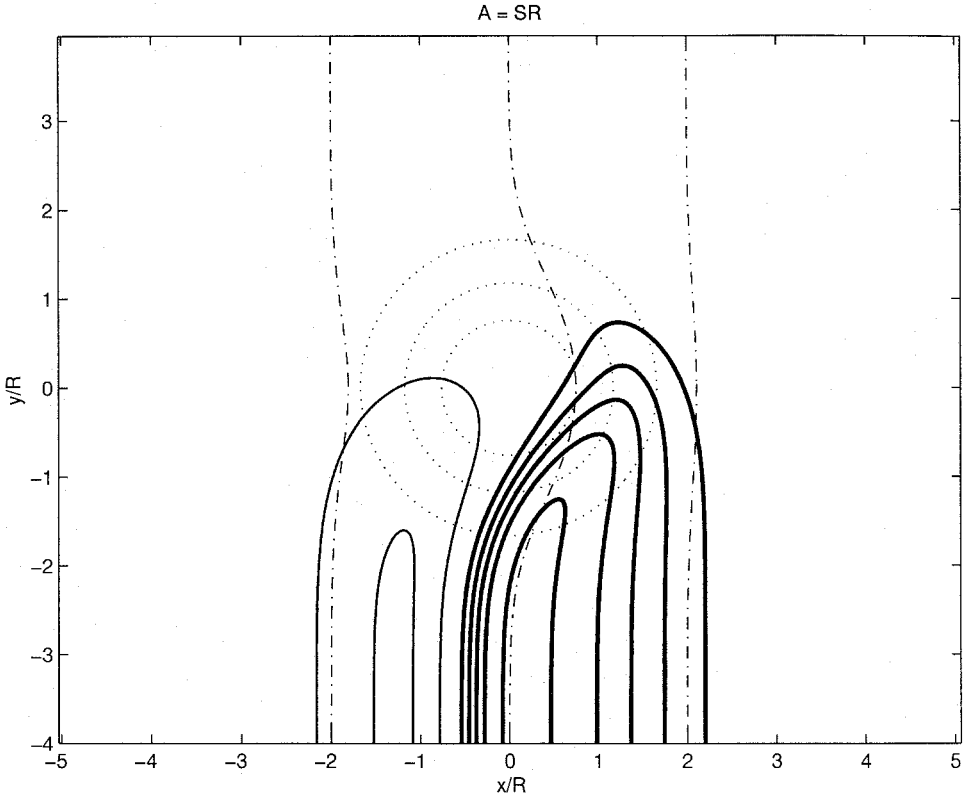

Figure 2. The second component of the lower-layer flow, F, described by (22) for a Gaussian vortex (26) with $A = SR$ superimposed by isolines of the interface, P, (dotted circles) and isolines of ζ (dash-dotted lines). Thick lines represent cyclonic circulation.

Sverdrup relation (see Section 5). For zonal bathymetry, $\cos\theta = 0$, the westward beta-induced along-slope vortex motion is affected only by the slope variation as described below.

b. Variable slope

The effect of a variable slope on the cross-slope propagation speed can also be assessed from the integral constraints in the case of steep slope ($|P'| \ll dH/dx$). First, we divide (12) by dH/dx and assume that

$$\left(\frac{dH}{dx}\right)^{-1} = \frac{1 + \mu x}{S} \tag{27}$$

where S is the mean slope steepness, and the coefficient μ describes the curvature of the ocean depth (the slope steepness increases onshore if $\mu > 0$). Then we multiply (12) by $P - P_\infty$ and integrate over the plane taking into account that $|P'| \ll dH/dx$ to obtain

$$\int P\partial_y \psi dxdy = -\dot{x}_0 \frac{\mu E_p}{S}. \tag{28}$$

Inserting (28) into (18) for the cross-slope speed we obtain

$$\dot{x}_0 = -\lambda \cos\theta\left(1 + \frac{E}{M}\right), \quad \lambda = \left(1 - \frac{\mu E_p}{SM}\right)^{-1}. \tag{29}$$

From this expression we see that when the slope increases onshore ($\mu > 0$), the cross-slope propagation speed of anticyclones ($E_p/M > 0$) is less than in the RG model ($\lambda < 1$), while the cross-slope speed of cyclones ($E_p/M < 0$) is larger than in the RG model ($\lambda > 1$). This effect is reversed when the slope steepness decreases onshore.

To see the effect of variable slope to the along-slope propagation, we can write an approximate solution to (12) as follows

$$\psi = \frac{1 + \mu x}{S}[\dot{y}_0(P(r) - P_\infty) - \dot{x}_0 F(x, y)], \tag{30}$$

where F is described by (25). Therefore,

$$\frac{1}{M}\int P\partial_x \psi dxdy = \dot{y}_0 \frac{\mu E_p}{MS} + \dot{x}_0 \frac{S_P}{S} \tag{31}$$

so that

$$\dot{y}_0 = \lambda\left[-\sin\theta\left(P_\infty + \frac{E}{M}\right) + \dot{x}_0 \frac{S_p}{S}\right]. \tag{32}$$

Comparing (32) with (29), we see the slope variation affects both the cross-slope and along-slope drift speeds in the same manner.

5. Discussion and conclusions

We have considered the effects of bathymetry on the propagation of intense, surface-intensified vortices in the two-layer model. A perturbation theory is suggested for the circular vortex with the lower layer at rest as a basic state. The vortex propagation speed is found from the integral relations which describe the beta-drift in the RG-approximation and an additional advection due to the lower-layer flow generated by the stretching effects. The most essential part of the lower-layer flow pattern can be explained in terms of potential vorticity conservation. The stretching in the lower layer associated with beta-induced cross-slope vortex interface migration should be balanced by a cross-slope water advection generating along-slope elongated dipolar gyres. They penetrate in the upper layer due to hydrostatic relation (4) and provide additional along-slope vortex drift.

The effects of mean slope and the slope variation can be described separately. The mean

slope effects produce an additional along-slope propagation which is proportional to the cross-slope drift speed and the ratio of the interface slope to the mean topographic slope. The mean slope does not affect the cross-slope drift which remains proportional to the along-slope component of the beta-drift in the RG-approximation. Slope variation modifies both along-slope and cross-slope drift speeds. The slope increasing onshore results in faster drift of cyclones and slower drift of anticyclones. The effect of the slope decreasing onshore is reversed.

Thus, for an arbitrary slope orientation the topographic effects can be evaluated in three steps. First, we decompose the beta-drift velocity obtained in the RG model into cross-slope and along-slope components. Second, we estimate a modification of the vortex drift due to slope variation beneath the vortex, this is described by the coefficient λ. Third, we calculate additional along-slope drift by multiplying the cross-slope drift by the coefficient which is proportional to the interface slope in the vortex and inversely proportional to the mean topographic slope.

For instance, when the Gulf Stream warm-core (anticyclonic) ring approaches the continental slope which is oriented roughly at $\theta = 45°$, the westward vortex beta-drift can be decomposed into nearly the same cross-slope and along-slope components ($\sin\theta = \cos\theta = \sqrt{2}/2$). Assuming for simplicity that the slope is constant and the ratio of the interface slope to the topographic slope is order one ($S_P \approx S$), from (23) we obtain nearly double along-slope drift due to the lower-layer gyres contribution. Thus, over the slope the west-southward ring drift is expected in agreement with observations (Smith, 1983; Evans *et al.,* 1985). Similar estimations can be obtained for other continental slopes with different orientation.

It should be emphasized that this simple theory is based on two main assumptions: (1) the radiation of topographic Rossby waves has adjusted lower-layer flow to the quasi-stationary state beneath the vortex and (2) the topographic slope is not smaller than the maximum interface slope; i.e. there are no closed isolines of the lower layer unperturbed thickness (this theory is not applied to the flat bottom case). The numerical investigation of the transition stage and the case of weak slope with closed isolines of lower-layer thickness is currently in progress and some examples are presented in Sutyrin *et al.* (2001). The results indicate that the perturbation theory adequately describes the main topographic effects, and the details of the numerical study will be reported in a future paper.

Acknowledgments. This work was supported by the USA National Science Foundation Grant #ATM-9905209 and the Office of Naval Research.

REFERENCES

Aiki, H. and T. Yamagata. 2000. Successive formation of planetary lenses in an intermediate layer. Geophys. Astrophys. Fluid Dyn., *92,* 1–29.

Benilov, E. S. 1996. Beta-induced translation of strong isolated eddies. J. Phys. Oceanogr., *26,* 2223–2229.

——— 2000. The dynamics of a near-surface vortex in a 2-layer ocean on the beta-plane. J. Fluid Mech., *420,* 277–299.

Carnevale, G. F., R. C. Kloosterziel and G. J. F. Van Heijst. 1991. Propagation of barotropic vortices over topography in a rotating tank. J. Fluid Mech., *233,* 119–139.

Cenedeze, C. and P. F. Linden. 1999. Cyclone and anticyclone formation in a rotating stratified fluid over a sloping bottom. J. Fluid Mech., *381,* 199–223.

Chassignet, E. P. and B. Cushman-Roisin. 1991. On the influence of a lower layer on the propagation of nonlinear oceanic eddies. J. Phys. Oceanogr., *21,* 939–957.

Dewar, W. K. and C. Gaillard. 1994. The dynamics of barotropically dominated rings. J. Phys. Oceanogr., *24,* 5–29.

Evans, R. H., K. S. Baker, O. B. Brown and R. C. Smith. 1985. Chronology of warm-core ring 82B. J. Geophys. Res., *90,* 8803–8811.

Firing, E. and R. C. Beardsley. 1976. The behavior of a barotropic eddy on a beta-plane. J. Phys. Oceanogr., *6,* 57–65.

Flierl, G. R. 1984. Rossby wave generation from a strongly nonlinear warm eddy. J. Phys. Oceanogr., *14,* 47–58.

——— 1987. Isolated eddy models in geophysics. Ann. Rev. Fluid Mech., *19,* 493–530.

Freeland, H. J., F. M. Boland, J. A. Church, A. J. Clarke, A. M. G. Forbes, A. Huyer, R. L. Smith, R. O. R. Y. Thompson and N. J. White. 1986. The Australian Coastal Experiment: A search for coastal-trapped waves. J. Phys. Oceanogr., *16,* 1230–1249.

Grimshaw, R., D. Broutman, Xinyu He and Pei Sun. 1994a. Analytical and numerical study of a barotropic eddy on a topographic slope. J. Phys. Oceanogr., *24,* 1587–1607.

Grimshaw, R., Y. Tang and D. Broutman. 1994b. The effect of vortex stretching on the evolution of barotropic eddies over a topographic slope. Geophys. Astrophys. Fluid Dyn., *76,* 43–71.

Hamon, B. 1965. The East Australian Current 1960–1964. Deep-Sea Res., *12,* 899–921.

Hart, J. E. 1975. Baroclinic instability over a slope. Part I: Linear theory. J. Phys. Oceanogr., *5,* 625–633.

Kamenkovich, V. M., Y. P. Leonov, D. A. Nechaev, D. A. Byrne and A. L. Gordon. 1996. On the influence of bottom topography on the Agulhas Eddy. J. Phys. Oceanogr., *26,* 622–643.

Killworth, P. D. 1983. On the motion of isolated lenses on a beta-plane. J. Phys. Oceanogr., *13,* 368–376.

——— 1986. On the propagation of isolated and multilayer and continuously stratified eddies. J. Phys. Oceanogr., *16,* 709–716.

Kirwan, A. D. Jr., J. K. Lewis, A. W. Indest, P. Reinersman and I. Quintero. 1988. Observed and simulated kinematic properties of Loop Current rings. J. Geophys. Res., *93,* 1189–1198.

Korotaev, G. K. 1997. Radiating vortices in geophysical fluid dynamics. Surveys in Geophys., *18,* 567–619.

LaCasce, J. H. 1998. A geostrophic vortex over a slope. J. Phys. Oceanogr., *28,* 2362–2381.

Louis, J. P. and P. S. Smith. 1982. The development of the barotropic radiation field of an eddy on a slope. J. Phys. Oceanogr., *12,* 56–73.

McDonald, N. R. 1998. The motion of an intense vortex near topography. J. Fluid Mech., *367,* 359–377.

Mory, M. 1985. Integral constraints on bottom and surface isolated eddies. J. Phys. Oceanogr., *15,* 1433–1438.

Mory, M., M. E. Stern and R. W. Griffiths. 1987. Coherent baroclinic eddies on a sloping bottom. J. Fluid Mech., *183,* 45–62.

Nezlin, M. V. and G. G. Sutyrin. 1994. Problems of simulation of large, long-lived vortices in the atmospheres of the giant planets (Jupiter, Saturn, Neptune). Surveys in Geophys., *15,* 63–99.

Nof, D. 1983a. The translation of isolated cold eddies on a sloping bottom. Deep-Sea Res., *30,* 171–182.

——— 1983b. On the migration of isolated eddies with application to Gulf Stream Rings. J. Mar. Res., *41,* 399–425.

——— 1985. Joint vortices, eastward propagating eddies and migratory Taylor columns. J. Phys. Oceanogr., *15,* 1114–1137.

Nycander, J. and G. G. Sutyrin. 1992. On the structure of stationary translating anticyclones on the beta-plane. Dyn. Atmos. Oceans, *16,* 473–498.

Pakyari, A. and J. Nycander. 1996. Steady two-layer vortices on the beta-plane. Dyn. Atmos. Oceans, *25,* 67–86.

Reznik, G. M. and W. K. Dewar. 1994. An analytic theory of distributed axisymmetric barotropic vortices on the β-plane. J. Fluid Mech., *269,* 301–321.

Reznik, G. M., R. Grimshaw and E. S. Benilov. 2000. On the long-term evolution of an intense localized divergent vortex on the beta-plane. J. Fluid Mech., *422,* 249–280.

Reznik, G. M. and G. G. Sutyrin. 2001. Baroclinic topographic modons. J. Fluid Mech., *437,* 121–142.

Richardson, G. 2000. Vortex motion in shallow-water with varying bottom topography and zero Froude-number. J. Fluid Mech., *411,* 351–374.

Sakamoto, T. and T. Yamagata. 1997. Evolution of baroclinic planetary eddies over localized bottom topography in terms of JEBAR. Geophys. Astrophys. Fluid Dyn., *84,* 1–27.

Shi, C. and D. Nof. 1994. The destruction of lenses and generation of wodons. J. Phys. Oceanogr., *24,* 1120–1136.

Smith, D. C. IV. 1986. A numerical study of Loop Current eddy interaction with topography in the western Gulf of Mexico. J. Phys. Oceanogr., *16,* 1260–1272.

Smith, D. C. IV and J. J. O'Brien. 1983. The interaction of a two-layer isolated mesoscale eddy with bottom topography. J. Phys. Oceanogr., *13,* 1681–1697.

Smith, P. C. 1983. Eddies and coastal interactions, *in* Eddies in Marine Science, A. R. Robinson, ed., Springer-Verlag, NY, 446–480.

Sutyrin, G. G. 1987. The beta-effect and the evolution of a localized vortex. Sov. Phys. Dokl., *32,* 791–793.

Sutyrin, G. G. and W. K. Dewar. 1992. Almost symmetric solitary eddies in two-layer models. J. Fluid Mech., *238,* 633–656.

Sutyrin, G. G. and G. R. Flierl. 1994. Intense vortex motion on the beta-plane. Development of the beta-gyres. J. Atmos. Sci., *51,* 773–790.

Sutyrin, G. G. and Y. Morel. 1997. Intense vortex motion in a stratified fluid on the beta-plane: an analytical theory and its validation. J. Fluid Mech., *336,* 203–220.

Sutyrin, G., D. Rowe, L. Rothstein and I. Ginis. 2001. Baroclinic-eddy interactions with continental slopes and shelves. J. Phys. Oceanogr., (in press).

Swaters, G. E. 1998. Dynamics of radiating cold domes on a sloping bottom. J. Fluid Mech., *364,* 221–251.

Swaters, G. E. and G. R. Flierl. 1991. Dynamics of ventilated coherent cold eddies on a sloping bottom. J. Fluid Mech., *223,* 565–587.

Thierry, V. and Y. Morel. 1999. Influence of a strong bottom slope on the evolution of a surface-intensified vortex. J. Phys. Oceanogr., *29,* 911–924.

Van Geffen J. H. G. M. and P. A. Davies. 1999. Interaction of a monopolar vortex with a topographic ridge. Geophys. Astrophys. Fluid Dyn., *90,* 1–41.

Van Heijst, G. J. F. 1994. Topography effects on vortices in a rotating fluid. Mecanica, *29,* 431–451.

Velasko Fuentes, O. U. and G. J. F. Van Heijst. 1994. Experimental study of dipolar vortices on a topographic β-plane. J. Fluid Mech., *259,* 76–106.

Vukovich, F. M. and E. Waddell. 1991. Interaction of a warm ring with the western slope in the Gulf of Mexico. J. Phys. Oceanogr., *21,* 1062–1074.

Whitehead, J. A., M. E. Stern, G. R. Flierl and B. A. Klinger. 1990. Experimental observations of baroclinic eddies on a sloping bottom. J. Geophys. Res., *95,* 9585–9610.

Received: *27 March, 2001;* revised: *28 August, 2001.*